International Journal of Advanced Science and Technology
Vol. 29, No. 9s, (2020), pp. 1383-1402

Integrating PV Systems with Battery Energy Storage Systems into Malaysian Medium Voltage Reference Networks for the Applications of PV Power Smoothing and Energy Time Shift

Hayder Salah Mohammed , Chin Kim Gan , MR Ab Ghani
Faculty of Electrical Engineering, Universiti Teknikal Malaysia Melaka (UTeM)
haydersalah11@yahoo.com [1], ckgan@utem.edu.my [2], dpdruddin@utem.edu.my [3]

Abstract

It is important for integrating Photovoltaic (PV) systems with battery energy storage in the distribution network for the enablement of continued uptake of PV system installations. The escalating interest pertaining the environmental and climatic change concerns has encouraged the integration of renewable resources such as PV system into power distribution networks worldwide, which will be essential towards the achievement of a sustainable future. The PV systems development has resulted in a number of concerns which include intermittency of supply, reverse power flow, and voltage rises. Hence, this paper compares the various techniques for solar power smoothing. Moreover, two kinds of BESS models were used in charging the distributed storage units during midday, of which the power from the solar PV would be higher than the load level. The energy that is stored is next utilized for the reduction of the peak load in the evening and early morning. Urban and Rural Malaysian medium voltage Reference Networks (RNs) have been considered, the effect of various configurations of PV systems have been offset with Battery Energy Storage Systems (BESS). From this, combinations of PV and storage that are most effective at mitigating the issues were explored.

Keywords*: Photovoltaic (PV), Battery Energy Storage System (BESS), PV power smoothing, energy time shift, Reference Network (RN).*

I. Introduction

The linking of electrical grids to the energy storage systems has shown increased quantitative as well as qualitative advantages for maintaining an economic and reliable system. As mentioned in [1-3], the energy storage systems can serve in bulk energy supply through the utilization of energy time shift (arbitrage) application. Additionally, the energy storage system is able to support several ancillary services like the output power smoothing for renewable energy (RE) resources (PV/wind), regulation, load following, and voltage support.

The PV generation follows the day-to-day patterns and seasonal patterns that are in proportion to the local irradiance. There might arise discrepancy between the PV generation and the local demand for the built environment, for example, the yearly discrepancy for a 4.5 kW_p PV installation and the electrical load of an individual residence was discovered to be eighty-one percent [4]. Widén et al. [5] conducted a comparison on the ability of varying PV array orientations, demand-side management tools, and Battery Energy Storage (BESS) for the enhancement of the matching capability of distributed PV positioned at high-latitude regions. Based on outcomes, it is found that BESS is the optimum efficient technology for the shifting of the PV generation in addressing the demand load at high PV penetration levels. The majority of Renewable Energy (RE) technologies are often incorporated at the distribution stage due to the small generator sizes, in addition to the voltage they produce [6,7].

Through the integration of PV generation, it was observed that the voltage profile is enhanced as voltage drop across feeder segments decreases, as the result from the decreased power flow via the feeder. Moreover, in instances when the generation from PV is bigger than the local demand at the Point of Common Coupling (PCC) of the PV inverter, the excess power surges revert to the grid. The PV inverters surplus power might generate reverse power surges in the feeder, which in turn might develop an increase in voltage at the feeder. A conventional solar PV resources peak time is noon time, when the degree of the

ISSN: 2005-4238 IJAST
Copyright ⓒ 2020 SERSC

sun irradiance level is the most intense. However, the demand from customers is ordinarily lower at this hour of the day. At the Medium Voltage (MV) distribution feeder, there might be the occurrence of an increase in voltage due to the light load and peak PV generation during that period. There is the pertinent necessity for resolutions to be recommended in order to decrease in excess in voltage resulted by the PV, in order for the aimed penetration level be attained, and at the same time, adherence to the the system operation parameters is equally maintained. In the work by [8], it was suggested that the implementation of storage devices be integrated with PV systems, to keep the excess power from the PV array in the afternoon period. The fundamental objective of the work by [8] was to decrease the power loss as a resultant from the incapability of utilizing the generated power from PV. The unutilized energy can be kept in the battery storage locally, to be utilized during the peak load period.

The PV power smoothing is a significant implementation for energy storage. In documented works, different techniques were recommended for the smoothing of the power production by solar [9-14]. A moving average (MA) technique was recommended in [15,16]. They utilized the MA technique for mitigation purposes for the short-term fluctuation of photovoltaic (PV) power by employing BESS. Additionally, from work by [17], the MA technique utilized to manage the battery energy in decreasing the PV power changes. In [18] an Exponential Moving Average (EMA) technique using hydrogen storage system was employed. It provides greater weights on the latest values. In the duo MA and EMA, the distance of how long the averaging window decides the way the storage systems charge or discharge. In instances when the length of the window is great, it necessitates the storage systems to encompass the difference between the actual and smoothed powers, even though the changes is not obvious [19] [29]. According to [20], a fuzzy wavelet transform technique was utilized to smoothen the generations of wind and solar power by utilizing batteries. Based on work by [19], it suggested a technique for ramp-rate control of PV power fluctuations.

The current research will emphasize the introduction of Battery Energy Storage Systems (BESS) for the enhancement of fundamental concerns regarding of intermittency, voltage rise, heightening difference between midday and peak loads, in addition to reverse power flow. By employing DIgSILENT power factory to model Urban and Rural medium voltage (MV) RN_s, integrations of BESS and PV systems were modelled for the provision of the optimum mitigation efficiency in addressing the restricting concerns. In this paper, two smoothing techniques were considered: simple moving average technique and polynomial curve fitting technique. Furthermore, the energy time shift application supervisors the BESS energy in order for the battery to be discharged at the time of the peak-load situations and charged during surplus of PV power generation.

II. Solar Variability Profiles

The simulation is carried out using five different PV variability profiles comprising overcast day, moderate variability day, clear sky day, high variability day, and mild variability day generation profiles [21]. The irradiance of solar is categorized into a few different categories employing the clearness index (K_T) and variability index (VI). The equations to calculate the K_T and VI are by using the Equation (1) and Equation (2), respectively. The changes in VI and K_T will significantly affect the PV power output because the PV generation solely depends on the solar insolation. For this research, Figure 1 shows five different types of normalized solar variability PV data which were collected from the UTeM's weather station. All the collected data is in the 1-minute resolution which is considered as a high-resolution interval. The lowest VI is representing the clear sky day, which in a generation profile has the least fluctuation. The clear sky day delivers a very constant irradiance profiles and very little step fluctuations to irradiance through the daytime cycle. Conversely, the overcast day possesses a very low solar irradiance caused by the crossing clouds and broken clouds that minimize the PV generation.

$$K_T = \frac{I_t}{I_t^{EX}} \quad (1)$$

Where, I_t = Ground level irradiance, I_t^{EX} = The irradiance extraterrestrial.

ISSN: 2005-4238 IJAST
Copyright ⓒ 2020 SERSC

$$VI = \frac{\sum_{k=2}^{n} \sqrt{(GHI_k - GHI_{k-1})^2 + \Delta t^2}}{\sum_{k=2}^{n} \sqrt{(CSI_k - CSI_{k-1})^2 + \Delta t^2}} \quad (2)$$

Where, GHI_k = Vector of length n of global horizontal irradiance, CSI_k = Vector calculated of clear sky irradiance, Δt = Time interval in minutes.

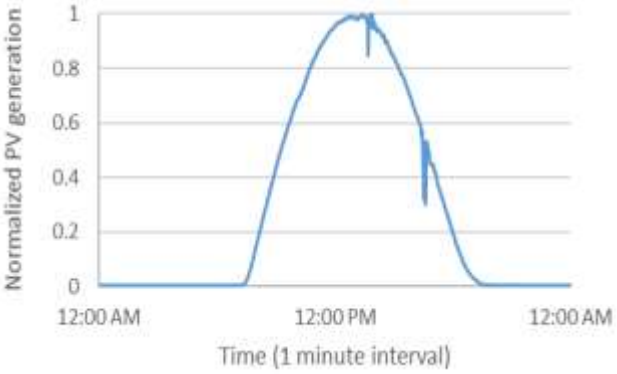

(a) Clear sky day (VI = 1.88) (K_T = 0.7)

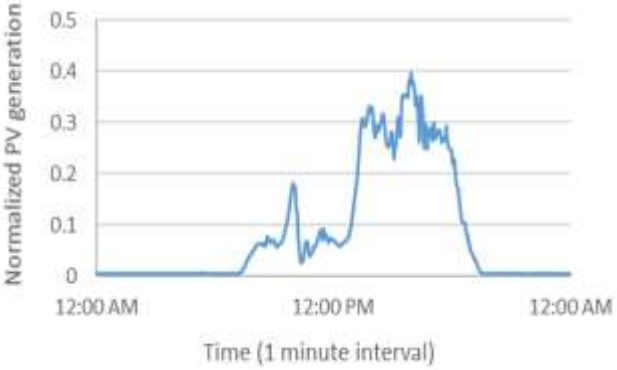

(b) Overcast day (VI = 1.33) (K_T = 0.2)

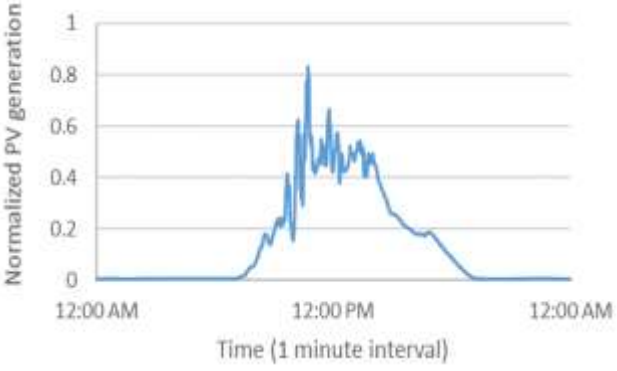

(c) Mild variability day (VI = 3.64)

ISSN: 2005-4238 IJAST
Copyright ⓒ 2020 SERSC

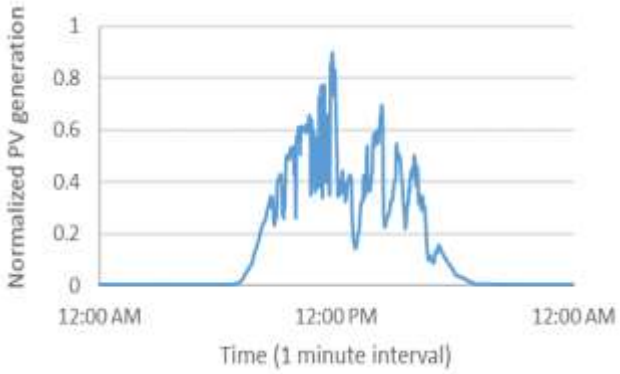

(d) Moderate variability day (VI = 7.72)

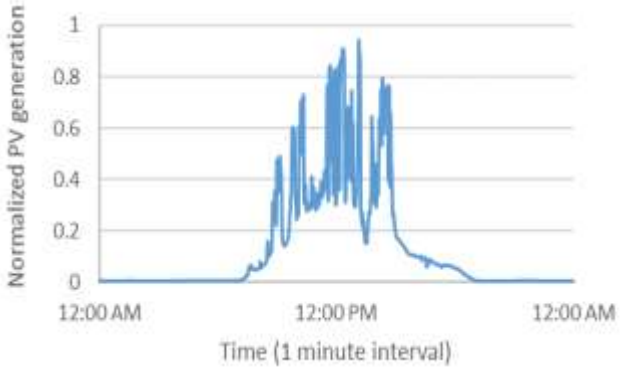

(e) High variability day (VI = 15.18)

Figure 1: Five different types of normalized solar variability PV data

III. System Topology

(a) Modeling of Reference Networks (RN_s)

Two reference networks were modeled, representing the real systems in the Malaysian networks. The reference networks were modeled by employing the generic characterization and parameters of RN in Malaysia that were attained from published works [22]. The software that was utilized to produce the models was the DIgSILENT power factory. One-minute time interval load flow simulations were performed on both RN_s models.

1) Urban RN with 33 and 11 kV feeders

The DIgSILENT model in Figure 2 illustrates the reference network for 132/33/11kV voltage transformation. There are two-voltage transformation stages in the model, which are from 132/33kV and 33/11kV primary substations. Table 1 depicts the development of the urban network parameters. Five 11kV feeders were linked to each of the 33/11kV transformer as indicated in Figure 2. Every 11kV feeder was individually linked to five 11/0.4kV transformers. Furthermore, 33/11kV and 11/0.4kV transformer capacities were calibrated to 30MVA and 1MVA, accordingly. In totality, the load for the low voltage transformer individually was 390kW with an assumed power factor of 0.90 lagging. The average distance was 600m, between the 11/0.4kV distribution transformers, where the average total length of individual 11kV feeder was 3km.

ISSN: 2005-4238 IJAST
Copyright ⓒ 2020 SERSC

Table 1: Parameters for urban RN with 33 and 11 kV feeders

Parameter	Value
132/33kV transformer capacity, MVA	45
No. of 11kV feeders per 33/11kV transformer	5
No. of 11kV transformer per 11kV feeder	5
Length 33kV line, km/each	5
33/11kV transformer capacity, MVA	30
11kV feeder length per feeder, km/each	3
11/0.4kV transformer capacity, MVA	1
Distance between TX 11/0.4kV, km/each	0.6
11/0.4kV transformer maximum demand, kW	390

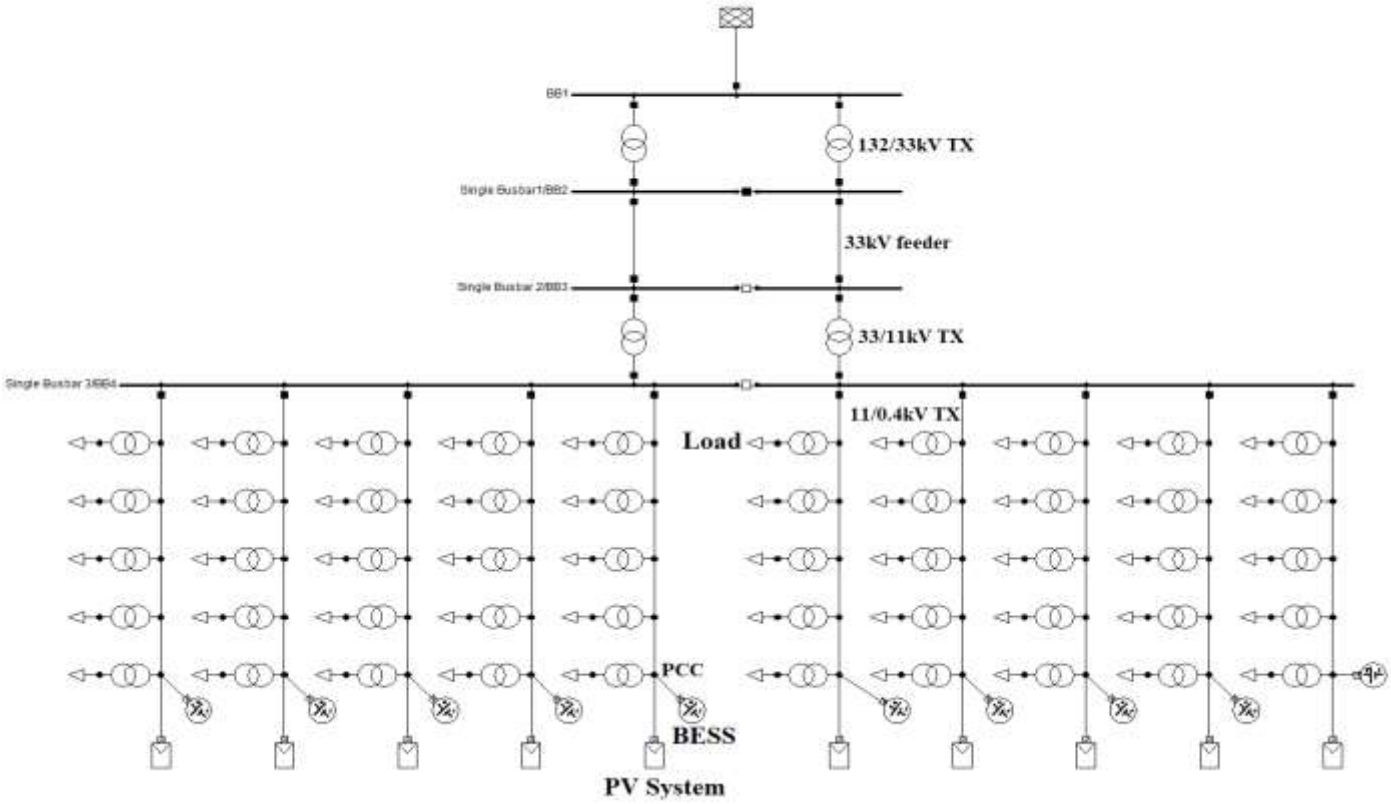

Figure 2: DIgSILENT model for urban RN with 33 and 11 kV feeders

2) Rural RN with 33 and 11 kV feeders

For rural network with 33kV and 11kV feeders, the model used was the DIgSILENT model as shown in Figure 3. Whereas, Table 2 indicates the rural network parameters. The maximum demand is 190kW for every individual 11/0.4kV transformer. The distance of the 33kV line from 30MVA rated 33/11kV transformer is extensively of greater length in comparison to urban RN, which is 18km. A single 11kV feeder that is 31.5km long is supplying 15 units of 11/0.4kV transformers. The length between each 0.5MVA rated 11/0.4kV transformer is 2.1 km.

ISSN: 2005-4238 IJAST
Copyright ⓒ 2020 SERSC

Table 2: Parameters for rural RN with 33 and 11 kV feeders

Parameter	Value
132/33kV transformer capacity, MVA	45
No. of 11kV feeders per 33/11kV transformer	3
No. of 11kV transformer per 11kV feeder	15
Length 33kV line, km/each	18
33/11kV transformer capacity, MVA	30
11kV feeder length per feeder, km/each	31.5
11/0.4kV transformer capacity, MVA	0.5
Distance between TX 11/0.4kV, km/each	2.1
11/0.4kV transformer maximum demand, kW	190

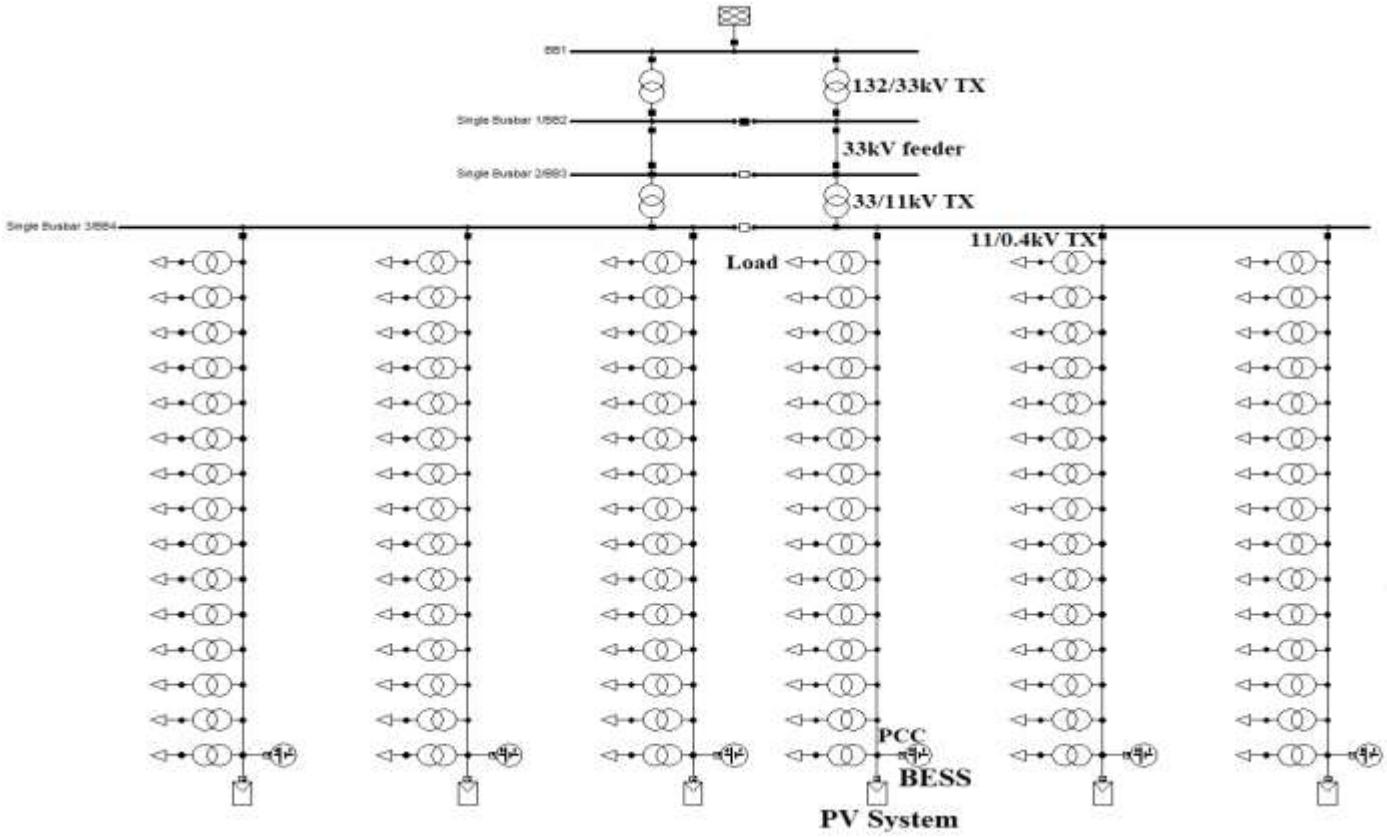

Figure 3: DIgSILENT model for rural RN with 33 and 11 kV feeders

(b) Modeling of PV System

Model PV system is designed by using 'ElmPVsys' function in DIgSILENT simulation software. In this research, PV system with unity power factor is categorised as a grid-tied inverter type. The generation profile of PV datasets was collected from the PV system installed at Photovoltaic and Smart Grid (PVSG) research laboratory at UTeM. The PV system is connected on the same node as that of the BESS as shown in Figure 2 and Figure 3.

ISSN: 2005-4238 IJAST
Copyright ⓒ 2020 SERSC

(c) Modeling of Battery Energy Storage System (BESS)

Battery energy storage enables the integration of greater amounts of PV system generation through the smoothening power output, time shifting generated energy to follow demand, and reducing the voltage rise. BESS is also modeled through the utilization of 'ElmGenstat' and 'ElmQdsl' functions in DIgSILENT power factory software. The battery minimum, maximum, and initial SOC is typically set to 10%, 90%, and 20%, respectively, in order to avoid damaging the storage bank. Moreover, the battery SOC is calculated through Equation (3). The charging power of BESS is shown by the (-) symbol and the discharging power of BESS is shown by the (+) symbol, accordingly. For the current study, a lithium ion battery-based storage system was chosen. Both PV system and BESS was linked to the single point of common coupling (PCC) for the purpose of simulation. The parameters used in the BESS power and voltage models are shown in Tables 3 and 4, respectively. BESS power model is used to follow the load by charging during surplus of PV power generation and discharge when demand is higher than generation, while BESS voltage model is used to mitigate the voltage rise issue.

$$\mathrm{SOC(t)} = \mathrm{SOC(t-1)} + \int_0^t \frac{I}{C_{bat}}\, dt \times 100\% \qquad (3)$$

Where, SOC(t): Battery state of charge at time t (%), SOC(t-1): Battery initial state of charge (%), I: Charge/discharge current (A), t: Time (h), C_{bat}: Battery capacity.

Table 3: Parameters used in the BESS power model

Parameter	Value
Eini Storage energy size [MWh]	8.253
SOCini Initial state of charge [%]	20
SOCmin Minimal state of charge [%]	10
SOCmax Maximal state of charge [%]	90
Pstore Nominal storing active power [MW]	1.258
Qstore Nominal storing reactive power [Mvar]	0
PFullStore Power to store at full power [MW]	1.258
PStartStore Power to start storing [MW]	0.001
Pfeed Nominal feeding active power [MW]	1.258
Qfeed Nominal feeding reactive power [Mvar]	0
PStartFeed Power to start feeding [MW]	0.934
PFullFeed Power to feed at full power [MW]	1.967
Orientation 1=terminal j is closest, otherwise -1	1

ISSN: 2005-4238 IJAST
Copyright ⓒ 2020 SERSC

Table 4: Parameters used in the BESS voltage model

Parameter	Value
Eini Storage energy size [MWh]	7.826
SOCini Initial state of charge [%]	20
SOCmin Minimal state of charge [%]	10
SOCmax Maximal state of charge [%]	90
Pstore Nominal storing active power [MW]	1.235
Qstore Nominal storing reactive power [Mvar]	0
uFullStore Voltage to store at full power [p.u.]	1.06
uStartStore Voltage to start storing [p.u.]	1.05
Pfeed Nominal feeding active power [MW]	1.235
Qfeed Nominal feeding reactive power [Mvar]	0
uStartFeed Voltage to start feeding [p.u.]	1.021
uFullFeed Voltage to feed at full power [p.u.]	0.94

(d) Modeling of Network Demand

It extremely complex and problematic to identify all the types of customers served by each distribution transformer during the procedure of feeder analysis for a distribution system. To solve this problem, the solution is to develop a set of composite load profiles employing typical load data obtained from the power utility. Figure 4 indicates the typical load profiles of residential, commercial, and industrial customers [23]. In addition, all the loads modeled in DIgSILENT has power load with power factor equal to 0.90. The developments of the two reference networks are constructed according to residential, commercial, and industrial demand profiles. The minimum and maximum load change according to each reference network because of different user mix in the network. The load factors for the residential, commercial, and industrial networks were computed as 0.465, 0.598, and 0.755, respectively.

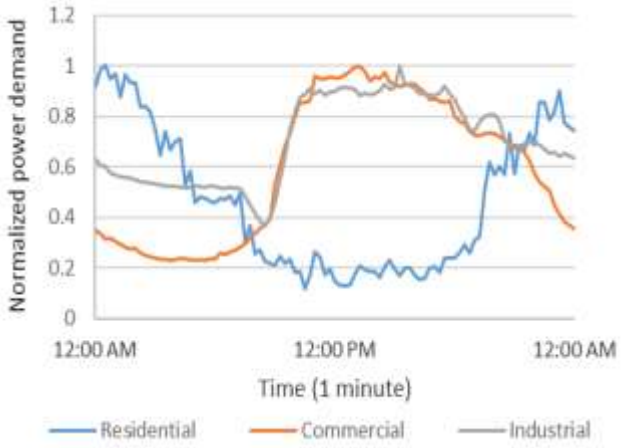

Figure 4: Typical load profiles of residential, commercial, and industrial customers

ISSN: 2005-4238 IJAST
Copyright ⓒ 2020 SERSC

IV. Methodology

(a) PV Power Smoothing

In this study, the adoption of simple moving average and polynomial curve fitting techniques are chosen to serve as the electric power smoothing techniques. The fundamental principle of these smoothing techniques is to smoothen the high fluctuations in the PV generated power, that is caused by partial shading of the PV arrays. The aforementioned smoothing techniques produce a battery power reference which mitigate the PV power variations at the point of common coupling (PCC). The total installed PV capacity on each of the MV lines for urban and rural networks is approximately 0.341 MW and 0.712 MW, respectively.

1) Simple Moving Average

Simple moving average technique used in [24,15] takes the past values of the PV power for a selected period of time w, finding the average value for it as shown in Equation (4), where n represents the current sampling value.

$$P_{ref-_{es}}(n) = \frac{\sum_{i=0}^{w-1} P_{pv}(n-i)}{w} - P_{pv}(n) \qquad (4)$$

Depending on whether the averaging period is large or small, the smoothing of the PV power will be more or less significant, respectively. This research proposes to use a 60-minute averaging interval to reduce power fluctuations. The more aggressive the smoothing, the more battery power will be needed, since they are between adjacent peaks has to filled by the energy from the storage.

2) Polynomial Curve Fitting

The curve fitting techniques are employed for the purpose of processing and extracting a mathematical relationship between the acquired data of PV output power [25]. The curve fitting defines an appropriate curve to fit the measured values and employs a curve function for the analysis of the relationship between the variables. The objective of curve fitting is to ascertain a function f(x) for the input measured data (x_i,y_i) where i = 1, 2,..,,n means the number of measurements. The general polynomial fits the data set to a polynomial function of the general form shown in Equation (5). In this study, six-order polynomial was used to provide a good fit to the data.

$$F(x) = a_0 + a_1 x + a_2 x^2 + \ldots\ldots\ldots \qquad (5)$$

(b) Energy Time Shift

Bulk energy storage is the repository of huge quantities of intermittent electricity when it is produced for the purpose of its utilization during low production periods, for example, storing solar energy during the midday for its utilization in the evening and early morning [26,27]. The stored energy can be discharged for varying applications. A probable application is to charge and discharge the storage unit to follow the system load, termed as load following. Another application of bulk energy storage is for the reduction of the voltage rise, where there is a necessity for the surplus quantity of power from the solar PV units to be lessened. The flowchart indicated in Figure 5 is utilized for the energy management of the simulated grid-connected PV system. Initially, the BESS model compiles the generated solar power (P_{solar}), required load (P_{load}) and also the SOC of the battery (SOC_{bat}). Following the serving of the required load, if there are excess of energy, it is then kept in the battery. However, for more quality in battery management, its SOC is restricted from exceeding 90%. In instances when the battery is completely charged, in the likelihood of the existence of extra energy, it is then sold to the grid. Conversely, in instances when the solar radiation is low, the generated power from PV is insufficient to supply the required load. Thus, alternative energy source is needed to address the load. In instances when the battery SOC is less than 10%, the required power ($P_{required} = P_{load} - P_{solar}$) is purchased from the grid. In the case that the battery SOC is higher than 10%, the required power may be discharge to the load from the storage battery. In order to properly

ISSN: 2005-4238 IJAST
Copyright ⓒ 2020 SERSC

manage the battery, its operations must be carefully handled, in order for its SOC not to be lower than 10%, as this is imperative. In instances that SOC goes lower than 10%, there arise an eventual risk on battery life. The total installed PV capacity on each of the MV lines for urban and rural networks will be approximately 1.755 MW and 2 MW, respectively.

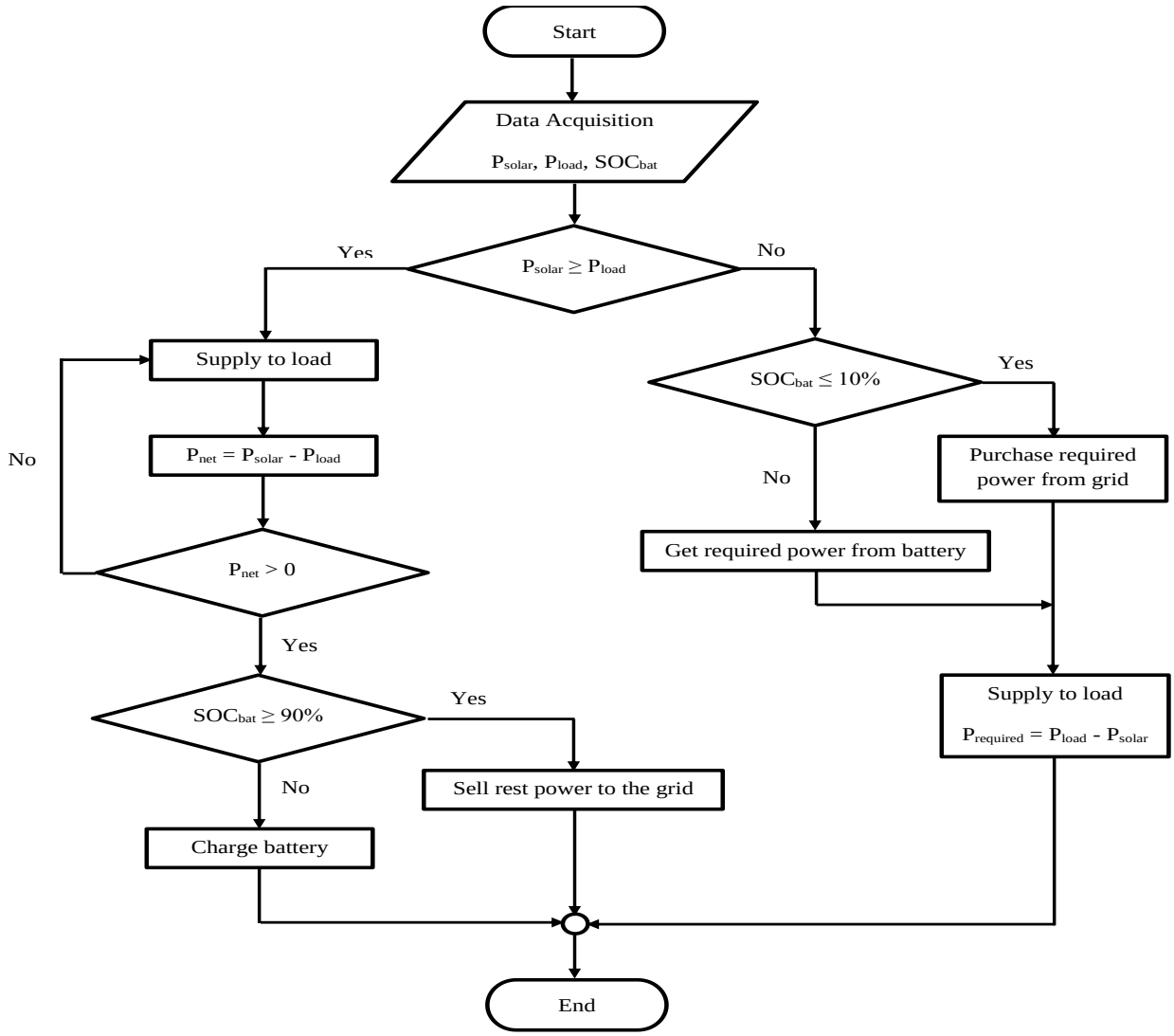

Figure 5: Flowchart of Battery Energy Storage System (BESS) model operation

V. Simulation Results

(a) PV Power Smoothing

The illustrations of the simulation results of the two PV power smoothing techniques with four varying PV variability profiles are illustrated in this section, comprising overcast day, moderate variability day, high variability day, and mild variability day generation profiles. The simulation considers the integrated BESS and PV system. The PV system is controlled to operate at unity power factor i.e. the reactive power output (Q_{PV}) is zero. The PV system output power with the sixth order polynomial and 60 min moving average smoothed curves are indicated by Figures from 6 to 9 (a). The BESS output power is indicated in Figures from 6 to 9 (b) & (c). The difference between the smoothed curve and actual power output curve is the battery power. Negative power signifies battery charge, meanwhile positive signifies discharge. The State of Charge (SoC) of the battery is configured to 20% at the start of the day to enable adequate energy

ISSN: 2005-4238 IJAST
Copyright ⓒ 2020 SERSC

charge and discharge ability for power smoothing. Table 5 shows maximum capacity of battery used to smooth the four different PV variability based on two smoothing techniques. It also shows that high PV variability need highest battery capacity to smooth it. This is due to the fact that high variability has the highest peak and trough of power. In this paper, high PV variability battery capacity was used to smooth all PV variability types at the Point of Common Coupling (PCC).

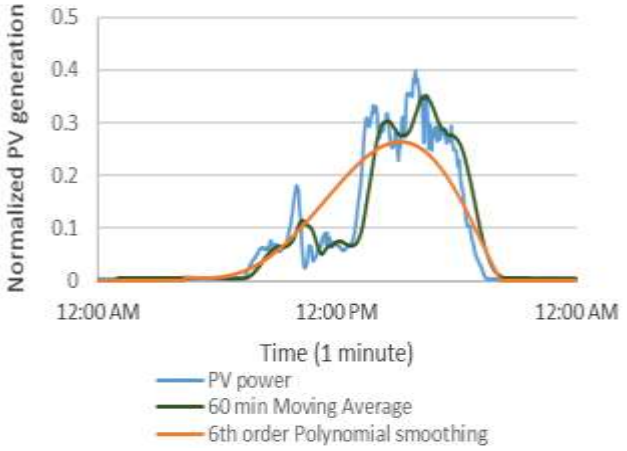

(a)

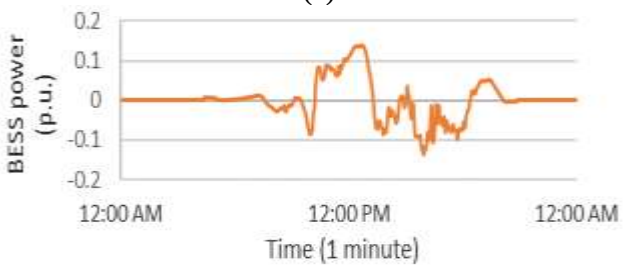

(b)

(c)

Figure 6: PV power smoothing simulation results for overcast day. (a) PV power output compared to polynomial and moving average smoothed curves. (b) & (c) BESS output power for moving average and polynomial smoothing.

ISSN: 2005-4238 IJAST
Copyright ⓒ 2020 SERSC

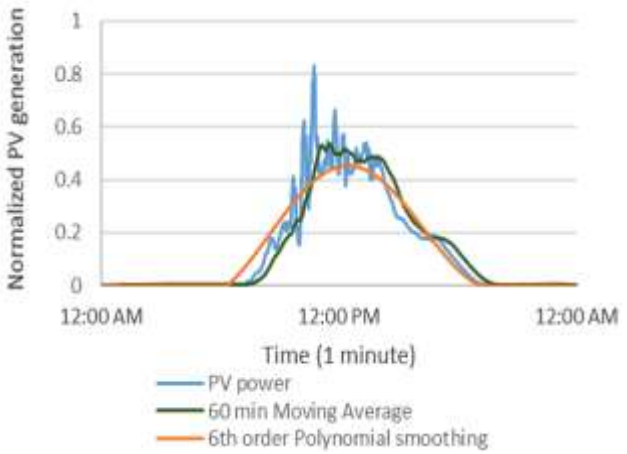

(a)

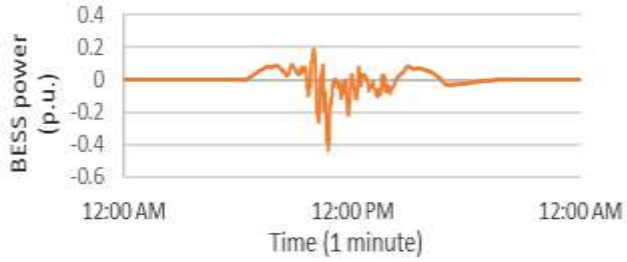

(b)

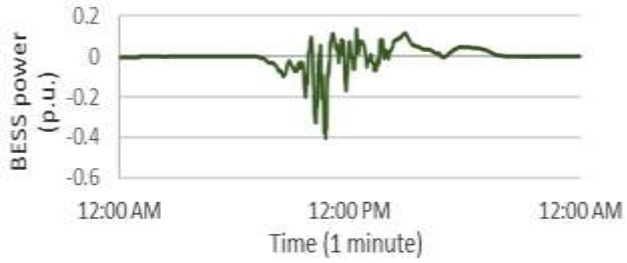

(c)

Figure 7: PV power smoothing simulation results for mild variability day. (a) PV power output compared to polynomial and moving average smoothed curves. (b) & (c) BESS output power for moving average and polynomial smoothing.

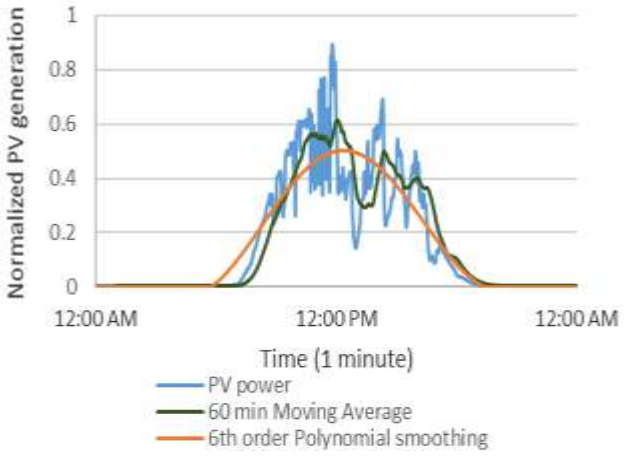

(a)

ISSN: 2005-4238 IJAST
Copyright ⓒ 2020 SERSC

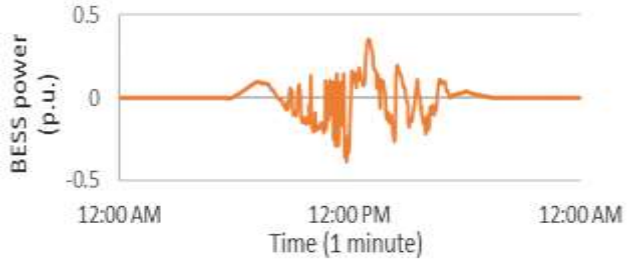

(b)

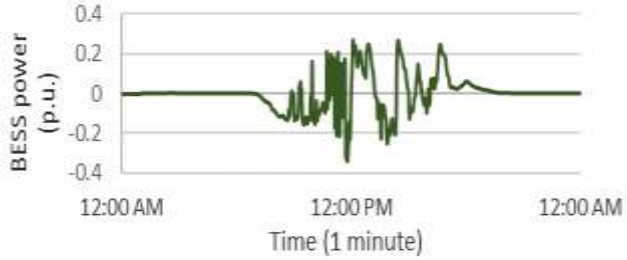

(c)

Figure 8: PV power smoothing simulation results for moderate variability day. (a) PV power output compared to polynomial and moving average smoothed curves. (b) & (c) BESS output power for moving average and polynomial smoothing.

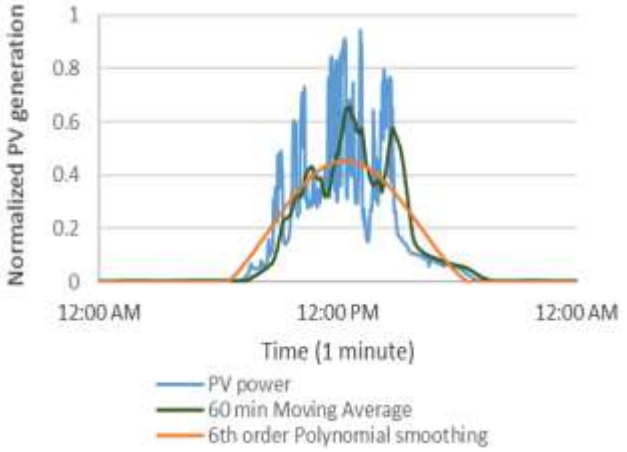

(a)

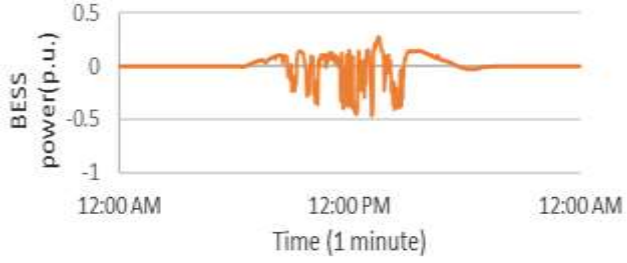

(b)

ISSN: 2005-4238 IJAST
Copyright ⓒ 2020 SERSC

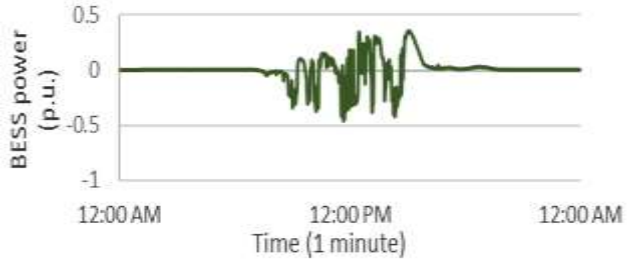

(c)

Figure 9: PV power smoothing simulation results for high variability day. (a) PV power output compared to polynomial and moving average smoothed curves. (b) & (c) BESS output power for moving average and polynomial smoothing.

Table 5: Maximum capacity of battery in p.u.

Battery capacity (p.u.)				
PV variability	Polynomial curve fitting technique		Simple moving average technique	
	Power (p.u.)	Energy (p.u.)	Power (p.u.)	Energy (p.u.)
Overcast	0.137	0.357	0.166	0.252
Mild variability	0.428	0.358	0.398	0.350
Moderate variability	0.384	0.626	0.345	0.615
High variability	0.472	0.718	0.459	0.704

(b) Comparison of Smoothing Techniques

The fundamental research goal is in the determination of the needed BESS capacity for utilization together with a PV power system which enables the output of the combined PV power system and BESS in fulfilling the connected grid necessities. This refers to the fluctuation of injected power to the grid that must be decreased for the improvement of the grid power quality. The comparison of smoothing techniques include: the simple moving average technique and the polynomial curve fitting technique. The criteria involved in the selection of the smoothing technique entail the power and energy capacities of the battery, the battery cost, the maximum demand, the standard deviation of the smoothed power, and the total annual cost of losses. The resultant energy capacities and power capacities of the different techniques are shown in Table 6 and Table 7, where the simple moving average technique requires lowest energy and power capacities of the battery in compared to the polynomial curve fitting technique. The cost of energy storage is usually expressed in two units: RM per kW and RM per kWh and calculated using Equation (6). The standard deviation of the smoothed power is defined in Equation (7), for a more extensive comparison of the smoothing performance of different smoothing techniques for power quality. The standard deviations of smoothed power of various smoothing techniques are indicated in Tables 6 and 7, where the polynomial curve fitting technique possesses the smallest value. Additionally, the cost of annual losses in the distribution system installations is shown in Equation (8). The cost of annual losses in the distribution system following the smoothing the PV output power employing the simple moving average technique and the polynomial curve fitting technique are shown in Tables 6 and 7, where the two techniques show the same values of annual losses. Finally, simulations show that, although the polynomial curve fitting technique has the smallest standard deviation, it requires the largest battery capacity and cost, and also it produces a highest maximum demand, causing it to be unfit with storage technologies as lithium-ion.

$$\text{Cost}_{\text{total}}(\text{RM}) = \text{Cost}_{\text{pcs}}(\text{RM}) + \text{Cost}_{\text{storage}}(\text{RM}) \qquad (6)$$

Where, $\text{Cost}_{\text{pcs}}(\text{RM}) = \text{Unit Cost}_{\text{pcs}}(\text{RM/kW}) \times \text{P (kW)}$, $\text{Cost}_{\text{storage}}(\text{RM}) = \text{Unit Cost}_{\text{storage}}(\text{RM/kWh}) \times (\text{E (kWh)} / \eta)$.

ISSN: 2005-4238 IJAST
Copyright ⓒ 2020 SERSC

$$\sigma = \sqrt{\frac{\sum_{i=1}^{h}(P_{pv}(t_i) - P_{out}(t_i))^2}{h}} \quad (7)$$

Where, σ: Standard deviation of the smoothed power, P_{pv}: Actual PV power, P_{out}: Smoothed PV power, h: Total number of sampling.

$$C_L = NL \times \sum_{t=1}^{8760} ep(t) \quad (8)$$

Where, C_L: Total annual cost of losses (RM/year), NL: Network energy losses (kWh), ep(t): Energy price in time period t (RM/kWh).

Table 6: Comparison of two smoothing techniques based on various criteria for Urban RN with 33 and 11kV feeders

Criteria	Polynomial curve fitting technique	Simple moving average technique
Power (MW)	0.161	0.157
Energy (MWh)	0.245	0.240
Battery cost (RM)	981172	959898
Max demand (MW)	1.95	1.93
σ (MW)	0.038	0.039
Cost of losses (RM/year)	575949.8	575949.8

Table 7: Comparison of two smoothing techniques based on various criteria for Rural RN with 33 and 11kV feeders

Criteria	Polynomial curve fitting technique	Simple moving average technique
Power (MW)	0.336	0.327
Energy (MWh)	0.511	0.501
Battery cost (RM)	2046543	2002170
Max demand (MW)	2.856	2.755
σ (MW)	0.079	0.082
Cost of losses (RM/year)	1554840	1554840

ISSN: 2005-4238 IJAST
Copyright ⓒ 2020 SERSC

(c) PV Energy Time Shift

1) Load Following

The DIgSILENT software was used to simulate the energy time shift for urban network, as this network experiences the problem of mismatch between the PV generation and the local demand. For the simulation of the worst case scenario e.g. in instances of low electricity demand, and solar energy production is at the highest point, a simulation of a clear sky day is conducted. In order to simulate a clear sky day, the needed battery power is 1.258 MW, and the needed battery capacity is 6.878 MWh. Figure 10 (a) indicates the active power of PV and load, plotted with PCC and net active power. At the times of uninterrupted days of sun and low consumption, the difference between electricity demand and PV system generation will be the largest, and hence the reverse power flow is anticipated to arrive at its maximum value. The BESS for load following charges once the PV system produces greater active power as compared to its consumption, and discharges in instances when the demand is greater in comparison to its generation. The charging profile for the BESS is indicated in Figure 10 (b). Moreover, the adoption of the State of Charge (SOC) estimation utilizing Coulomb counting technique is implemented for the management of the active power in the current research. Additionally, in battery energy management, the typical minimum and maximum SOC is 10% and 90%, respectively, as shown in Figure 10 (c). As observed from the net power curve in Figure 10 (a) the maximum demand decreased from 1.95 MW to 0.922 MW, showing a decrease of 52.71%.

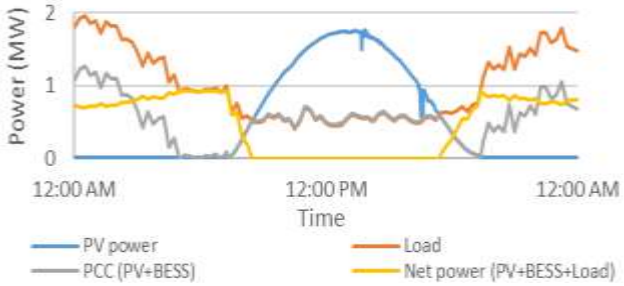

(a)

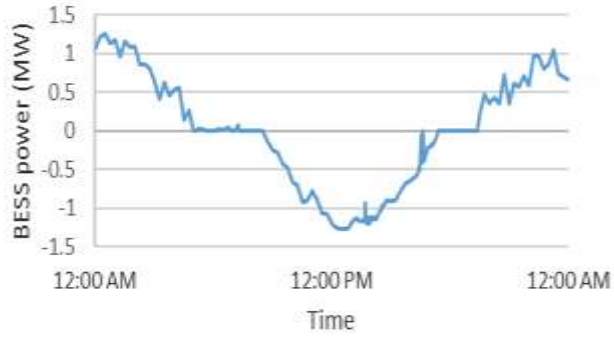

(b)

ISSN: 2005-4238 IJAST
Copyright ⓒ 2020 SERSC

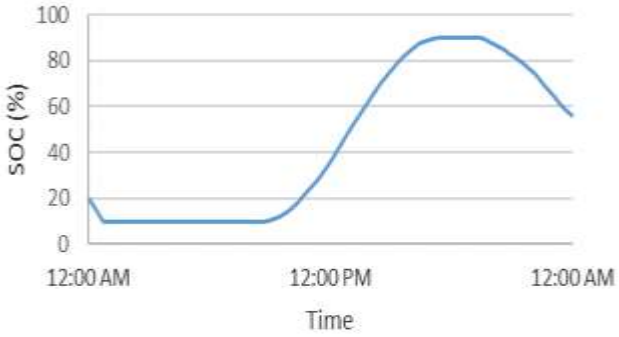

(c)

Figure 10: Energy time shift simulation results. (a) Active power of PV and load, plotted with PCC and net active power. (b) BESS output power. (c) Battery SOC.

2) Voltage Rise

In this section, PV energy time shift was performed on rural network, as this network experiences the problem of overvoltage due to reverse power flow, which is typically caused by high PV generation output under minimum load conditions. The steady-state voltage fluctuation under the normal condition on the medium voltage distribution network in Malaysia is (0.95-1.05 p.u.) ±5% of the nominal value [28]. In this part, a clear sky day generation profile was used with battery storage of 6.522 MWh will be integrated with each of the PV system unit in the 11kV feeder. Figure 11 (a) shows the active power of PV and load, plotted with PCC and net active power. For the purpose of the BESS simulation for voltage rise mitigation, the construction of the charging profile was for absorption of the active power that resulted in the increase of the voltage as indicated in Figure 11 (b) and is discharged in the evening and early morning time. The charging profile is indicated in Figure 11 (c). Through the absorption of the active power from the PV system based on the selected charging profile, the increases in voltage in the distribution grid that exceeded the permissible limit of 1.05 p.u. are prevented, as shown in Figure 11 (b). In addition, Figure 11 (d) shows the SOC profile for each 6.522 MWh BESS. It is observed from the net power curve in Figure 11 (a) that the maximum demand decreased from 2.856 MW to 1.698 MW, showing a decrease of 40.54%.

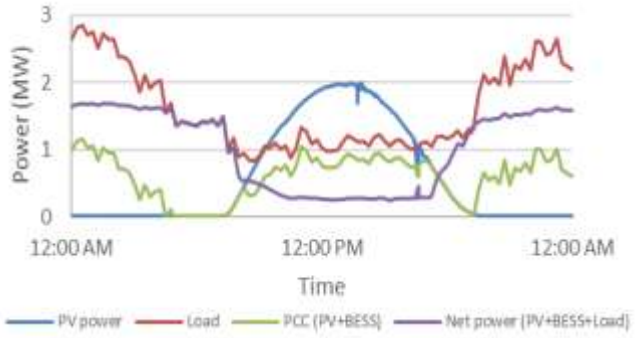

(a)

ISSN: 2005-4238 IJAST
Copyright ⓒ 2020 SERSC

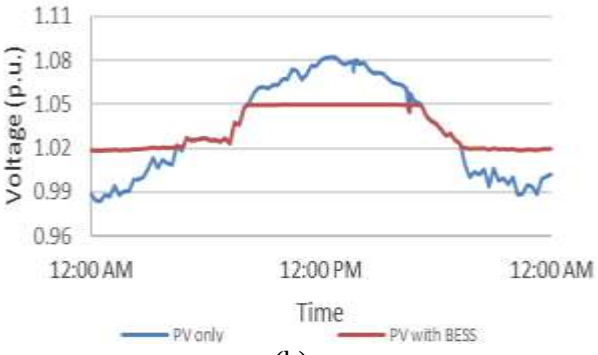

(b)

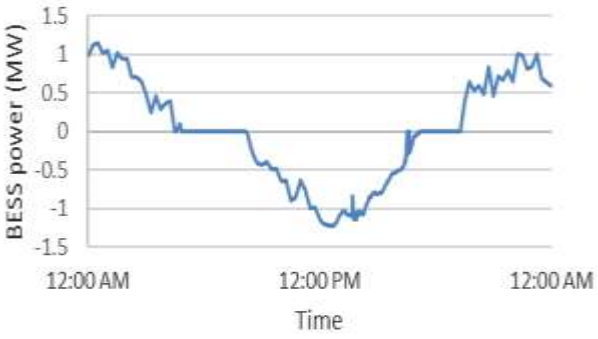

(c)

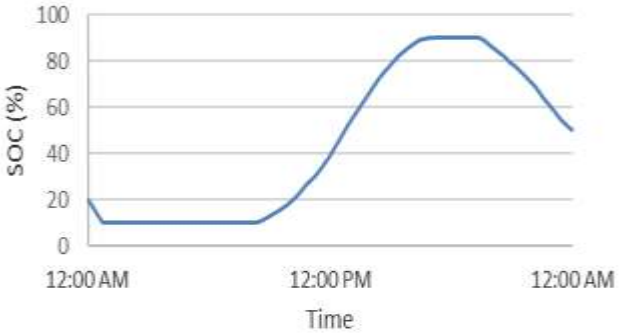

(d)

Figure 11: Energy time shift simulation results. (a) Active power of PV and load, plotted with PCC and net active power. (b) Voltage profile at PCC with and without BESS. (c) BESS output power. (d) Battery SOC.

VI. Conclusion

This paper presented a number of problems associated with high integration of distributed PV systems into Malaysian urban and rural MV reference networks. This includes supply intermittency, reverse power flow and voltage rises. The applications of energy storage for mitigating the issues caused by solar PV system has been presented. To mitigate the PV power fluctuation problem, two PV power smoothing techniques with four different PV variability profiles were considered. Furthermore, two types of BESS models were utilized to mitigate the reverse power flow and voltage rise issues. This research has made a comparative analysis on the simple moving average and the polynomial curve fitting techniques that were implemented to the electric power smoothing control for distributed generation systems. The simulation outcomes indicate that the simple moving average technique is much effective to decrease the PV power fluctuation in comparison to the polynomial curve fitting technique. The implementation results displayed

ISSN: 2005-4238 IJAST
Copyright ⓒ 2020 SERSC

led us to conclude that the devised PV power smoothing and energy time shift applications were successful in performing their respective functions.

Acknowledgement

Hayder Salah Mohammed wishes to extend his grateful appreciation to the UTeM Zamalah Scheme for offering his PhD scholarship.

References

[1] U. S. D. of Energy, "Grid Energy Storage," no. December, p. 67, 2013.
[2] M. Ahmed and S. Kamalasadan, "Energy storage PV capacity firming with forecasted power reference and optimal error minimization," *2015 North Am. Power Symp. NAPS 2015*, 2015.
[3] D. Parra, M. Gillott, S. A. Norman, and G. S. Walker, "Optimum community energy storage system for PV energy time-shift," *Appl. Energy*, vol. 137, no. September 2013, pp. 576–587, 2015.
[4] D. Parra, G. S. Walker, and M. Gillott, "Modeling of PV generation, battery and hydrogen storage to investigate the benefits of energy storage for single dwelling," *Sustain. Cities Soc.*, vol. 10, no. August 2012, pp. 1–10, 2014.
[5] J. Widén, E. Wäckelgård, and P. D. Lund, "Options for improving the load matching capability of distributed photovoltaics: Methodology and application to high-latitude data," *Sol. Energy*, vol. 83, no. 11, pp. 1953–1966, 2009.
[6] L. L. Freris and D. G. Infield, *Renewable energy in power systems*. John Wiley & Sons, 2008.
[7] N. S. Wade, P. C. Taylor, P. D. Lang, and P. R. Jones, "Evaluating the benefits of an electrical energy storage system in a future smart grid," *Energy Policy*, vol. 38, no. 11, pp. 7180–7188, 2010.
[8] Y. Ueda, K. Kurokawa, T. Tanabe, K. Kitamura, K. Akanuma, M. Yokota, and H. Sugihara, "STUDY ON THE OVER VOLTAGE PROBLEM AND BATTERY OPERATION FOR GRID-CONNECTED RESIDENTIAL PV SYSTEMS," *Mater. Japan*, vol. 46, no. 3, pp. 171–174, 2007.
[9] J. M. Eyer and G. P. Corey, "Energy storage for the electricity grid: benefits and market potential assessment guide," no. February, 2010.
[10] A. A. Hassan, W. Shah, A. M. Husein, M. S. Talib, A. A.-J. Mohammed, and M. Iskandar, 'Clustering Approach in Wireless Sensor Networks based on K-means: Limitations and Recommendations', *IJRTE*, vol. 7, no. 65, pp. 119–126, 2019.
[11] M. H. Albowarab, N. A. Zakaria, and Z. Z. Abidin, 'Smart DRILL Load Balancing Protocol : Wise Exploration and Reacting', *Int. J. Adv. Sci. Technol.*, vol. 28, no. 1, pp. 424–439, 2019.
[12] M. H. Albowarab, N. A. Zakaria, and Z. Z. Abidin, 'Software Defined Network : Architecture and Programming Language Survey', *Int. J. Pure Appl. Math.*, vol. 119, no. 18, pp. 561–572, 2018.
[13] A. Addisu, L. George, P. Courbin, and V. Sciandra, "Smoothing of renewable energy generation using Gaussian-based method with power constraints," *Energy Procedia*, vol. 134, pp. 171–180, 2017.
[14] S. Sukumar, M. Marsadek, K. R. Agileswari, and H. Mokhlis, "Ramp-rate control smoothing methods to control output power fluctuations from solar photovoltaic (PV) sources—A review," *J. Energy Storage*, vol. 20, no. April, pp. 218–229, 2018.
[15] A. Ellis, D. Schoenwald, J. Hawkins, S. Willard, and B. Arellano, "PV output smoothing with energy storage," *Conf. Rec. IEEE Photovolt. Spec. Conf.*, pp. 1523–1528, 2011.
[16] J. Johnson, A. Ellis, A. Denda, K. Morino, T. Shinji, T. Ogata, and M. Tadokoro, "PV output smoothing using a battery and natural gas engine-generator," *Conf. Rec. IEEE Photovolt. Spec. Conf.*, pp. 1811–1816, 2013.
[17] T. D. Hund, S. Gonzalez, and K. Barrett, "Grid-tied PV system energy smoothing," *Conf. Rec. IEEE Photovolt. Spec. Conf.*, pp. 2762–2766, 2010.

ISSN: 2005-4238 IJAST
Copyright ⓒ 2020 SERSC

[18] S. G. Tesfahunegn, Ø. Ulleberg, P. J. S. Vie, and T. M. Undeland, "PV fluctuation balancing using hydrogen storage - A smoothing method for integration of PV generation into the utility grid," *Energy Procedia*, vol. 12, no. 1876, pp. 1015–1022, 2011.

[19] M.J. Alam, K.M. Muttaqi, and D. Sutanto, "A Novel Approach for Ramp-Rate Control of Solar PV Using Energy Storage to Mitigate Output Fluctuations Caused by Cloud Passing," *IEEE Trans. ENERGY Convers.*, vol. 29, no. 2, pp. 507–518, 2014.

[20] X. Li, Y. Li, X. Han, and D. Hui, "Application of fuzzy wavelet transform to smooth wind/PV hybrid power system output with battery energy storage system," *Energy Procedia*, vol. 12, pp. 994–1001, 2011.

[21] K. A. Baharin, H. A. Rahman, M. Y. Hassan, C. K. Gan, and M. F. Sulaima, "Quantifying Variability for Grid-connected Photovoltaics in the Tropics for Microgrid Application," *Energy Procedia*, vol. 103, no. April, pp. 400–405, 2016.

[22] K. A. Bin Ibrahim, M. T. Au, and C. K. Gan, "Generic characteristic of medium voltage reference network for the Malaysian power distribution system," *2015 IEEE Student Conf. Res. Dev. SCOReD 2015*, pp. 204–209, 2015.

[23] K. A. Ibrahim, M. T. Au, C. K. Gan, and J. H. Tang, "System wide MV distribution network technical losses estimation based on reference feeder and energy flow model," *Int. J. Electr. Power Energy Syst.*, vol. 93, pp. 440–450, 2017.

[24] R. P. Sasmal, S. Sen, and A. Chakraborty, "Solar photovoltaic output smoothing: Using battery energy storage system," *2016 Natl. Power Syst. Conf. NPSC 2016*, 2016.

[25] S. A. Abdelrazek and S. Kamalasadan, "Integrated PV Capacity Firming and Energy Time Shift Battery Energy Storage Management Using Energy-Oriented Optimization," *IEEE Trans. Ind. Appl.*, vol. 52, no. 3, pp. 2607–2617, 2016.

[26] T. M. Jackson, G. R. Walker, and N. Mithulananthan, "Integrating PV systems into distribution networks with battery energy storage systems," *2014 Australas. Univ. Power Eng. Conf. AUPEC 2014 - Proc.*, no. September, 2014.

[27] S. Abdelrazek and S. Kamalasadan, "Integrated control of battery energy storage management system considering PV capacity firming and energy time shift applications," *2014 IEEE Ind. Appl. Soc. Annu. Meet. IAS 2014*, pp. 5–11, 2014.

[28] TNB, "TNB Technical Guidebook on Grid-interconnection of Photovoltaic Power Generation System to LV and MV Networks," pp. 1–46, 2013.

[29] M. Doheir, A. Kadhim, K. A. F. A. Samah, B. Hussin, and A. S. H. Basari, "Extension of NS2 framework for wireless sensor network," *Adv. Sci. Lett.*, vol. 20, no. 10–12, pp. 2097–2101, 2014.

ISSN: 2005-4238 IJAST
Copyright ⓒ 2020 SERSC